Printed in U.S.A.

66-WA/PT-8

an ASME publication

$1.50 PER COPY
75¢ TO ASME MEMBERS

The Effect of Hydrostatic Pressure (14kbar) on the Ultimate Compressive Strength of Various Sintered Materials[1]

THOMAS L. CORDELL

JAMES A. CORLL

Members, Technical Staff,
Sandia Laboratory,
Albuquerque, N. M.

This paper reports the investigation of the increase in ultimate compressive strength of sintered materials as a function of hydrostatic support pressures up to 14 kbar. Six tungsten carbide materials and five oxide ceramics were tested. All materials dispalyed significant increase in axial ultimate compressive strength when radically loaded by fluid pressure. For example: The ultimate compressive strength of WC with 3 percent Co binder is raised from 52 kbar to 92 kbar by 14 kbar fluid support pressure. A schematic design employing this effect in the design of a high-pressure apparatus is included.

[1]**This work was supported by the U. S. Atomic Energy Commission.**

Contributed by the Research Committee on Pressure Technology for presentation at the Winter Annual Meeting and Energy Systems Exposition, New York, N. Y., November 27-December 1, 1966, of The American Society of Mechanical Engineers. Manuscript received at ASME Headquarters, August 1, 1966.

Copies will be available until September 1, 1967.

THE AMERICAN SOCIETY OF MECHANICAL ENGINEERS, UNITED ENGINEERING CENTER, 345 EAST 47th STREET, NEW YORK, N.Y. 10017

The Effect of Hydrostatic Pressure (14kbar) on the Ultimate Compressive Strength of Various Sintered Materials

THOMAS L. CORDELL JAMES A. CORLL

INTRODUCTION

The strength of materials plays a prominent role in the design of most equipment and is especially important in the design of high-pressure apparatus. The maximum pressure obtainable in a simple piston-cylinder apparatus is limited to the ultimate compressive strength of the piston material. Higher pressures with a given material may be obtained by employing such techniques as the massive support principle (1)[2] used in Bridgman anvils and preloading with binding rings used in most solid medium devices (2). A third and more interesting means of raising the ultimate compressive strength of a piston is to radially support the piston while it is axially loaded. An excellent example of an apparatus employing this technique is the Kennedy (3) apparatus which radially supports the piston by pressure developed in the surrounding bismuth medium.

By considering the failure of a piston to be an energy-releasing process, one notes the ultimate compressive strength will be determined by tensile strains perpendicular to the applied load. Thus radial compressive loading will increase the ultimate axial compressive load the piston will withstand. By assuming the critical tensile strain to be a constant, one finds the increase in the ultimate compressive strength should be proportional to the radial loading divided by Poisson's ratio of the material. This implies the enhancement may be as high as three to four times the radial loading.

Bridgman employed these ideas when he built an apparatus within an apparatus (4) to increase his pressure range, and he also performed several experiments (5) to determine the effect of hydrostatic pressure on the ultimate compressive strength of materials. Considering the investigation of the phenomenon to be valuable, we have performed a series of similar experiments on larger samples at lower support pressures and obtained more detailed data.

[2] Numbers in parentheses designate References at the end of the paper.

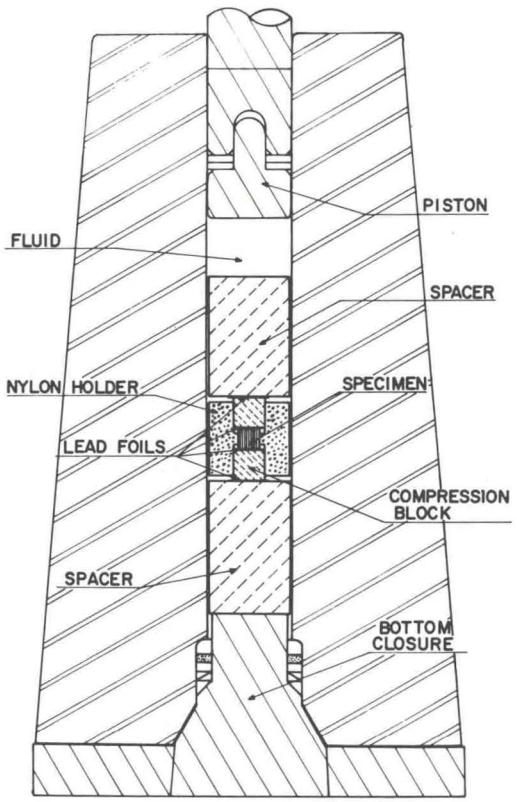

Fig. 1 Schematic representation of testing arrangement, piston travel monitoring device (not shown) was attached between press frame and piston of driving ram

In our experiments the ultimate compressive strengths of 11 brittle, low-compressibility materials were investigated as a function of hydrostatic support pressure using precision ground specimens 0.250 in. dia by 0.250 in. high.

EXPERIMENT

In most cases six specimens of each material were compressed to failure at six different hydrostatic support pressures ranging from 1 atm to

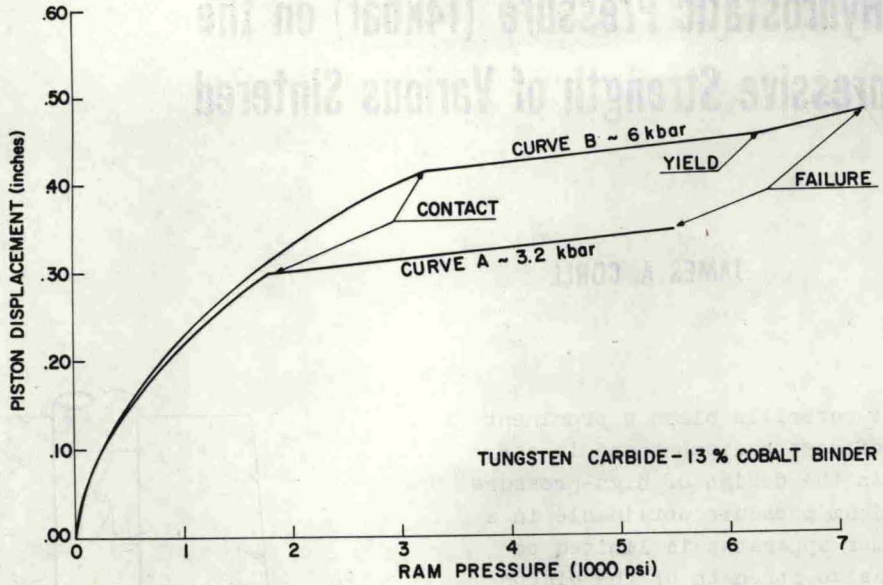

Fig. 2 Experimental data recorded during tests. Curve A typifies brittle failure and curve B typifies yielding before failure

14 kbar. All specimen surfaces were ground to at least a number sixteen finish with the ends plane and parallel. As shown in Fig.1, the specimens were compressed in a nylon holder between two tungsten-carbide compression blocks 0.375 in. in diameter. To reduce contact friction, and thereby minimize barreling, 0.001-in. lead foils were placed between the specimen and the compression blocks. The nylon holder guaranteed alignment of the sample in the pressure chamber and was shaped so that it provided no resistance to the compressive forces or radial support to the specimen.

The hydrostatic support pressures and the compressive forces were provided by the advancing piston of a commercial 30 kbar pressure apparatus (6). The advancing piston increased the hydrostatic support pressure by compressing the fluid (a mixture of n-pentane and isopentane) until contact was made with the tungsten-carbide spacers, Fig.1. Further advance of the piston applied the compressive loading to the specimen through the spacers and compression blocks. The hydrostatic pressure obtained before piston contact was varied by varying the length of the spacers.

During the experiments the pressure applied to the ram driving the piston and the displacement of the piston were continuously monitored on an x-y recorder. A marked change in slope of the piston displacement versus applied ram pressure curve occurred when the advancing piston contacted the spacers indicating the start of direct compressive loading. A discontinuous increase in the piston displacement indicated sample failure and was usually accompanied by an audible bang from within the pressure apparatus.

The pressure apparatus was calibrated at the start and at intermediate times during the course of this series of experiments. The applied ram pressure versus sample chamber hydrostatic-pressure calibration curve for the apparatus remained constant throughout the experiments and was determined by correlating the resistance of a manganin wire coil and applied ram pressure. The pressure coefficient of the manganin wire resistance was determined during the calibration experiments by the freezing pressure of mercury at room temperature.

DATA REDUCTION AND INTERPRETATION

The experimental data of two runs on specimens of 87 percent WC with 13 percent Co binder which are shown in Fig.2 are representative of the two types of failure encountered during the experiments. Curve A is typical of specimens which exhibited brittle failure without yielding and curve B is typical of specimens which yielded before failure. Note that in Fig.2, both specimens were of the same material and that, with sufficient hydrostatic support pressure, the normally brittle material exhibited yield and considerable deformation before failing. All experimental data curves displayed approximately the same slope after the piston contacted the spacers. Referring to curve A of Fig.2, over 90 percent of the displayed piston displacement between the contact point and the failure point can be ac-

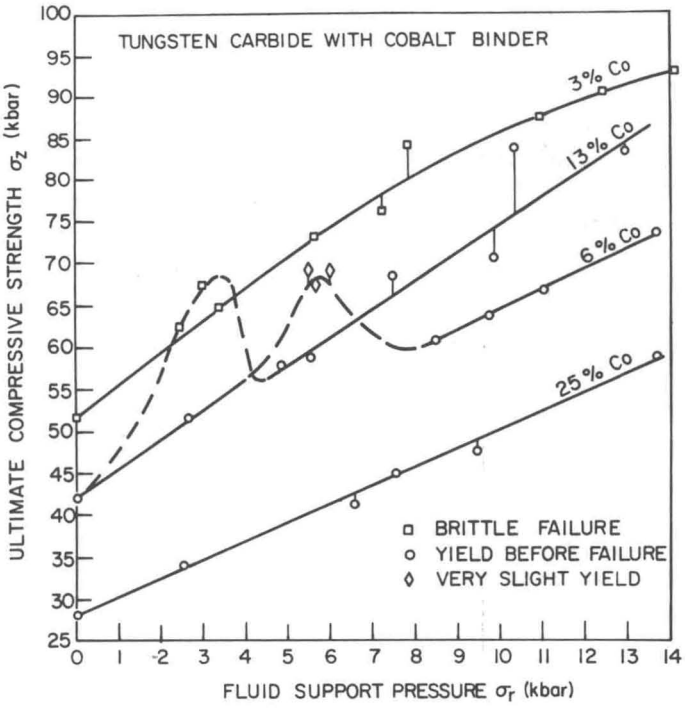

Fig. 3 Variation of ultimate compressive strength as a function of fluid support pressure for tunsten-carbide materials with cobalt binder

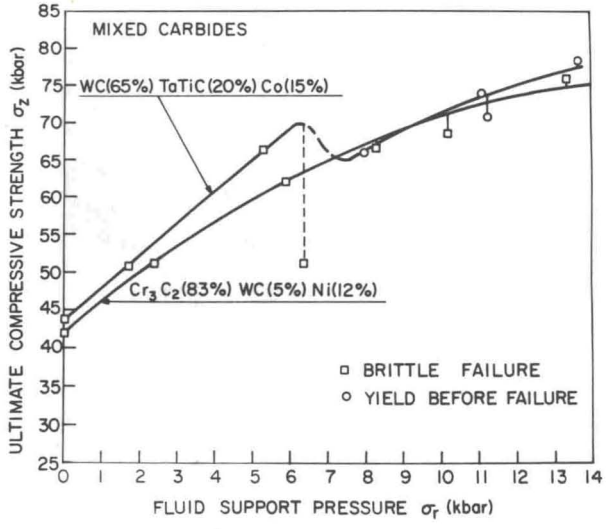

Fig. 4 Variation of ultimate compressive strength as a function of fluid support pressure for two mixed carbide materials

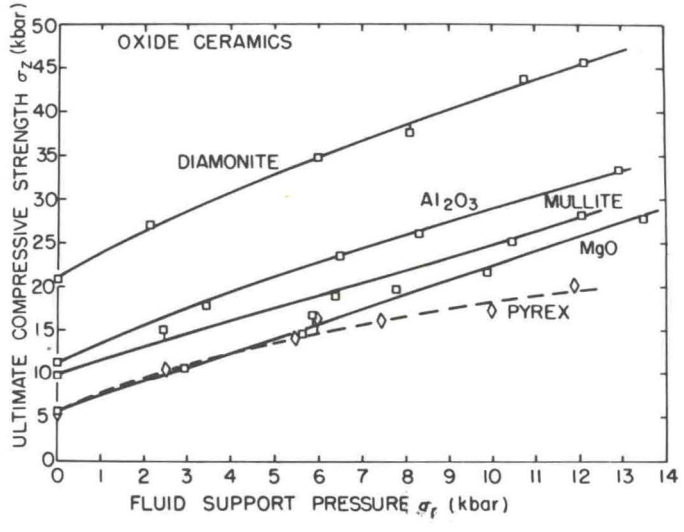

Fig. 5 Variation of ultimate compressive strength as a function of fluid support pressure for various oxide ceramics

counted for by considering the linear compression of the component parts (spacers, piston, seals, and driving ram) of the travel monitoring system. The relative changes in length of the specimens were small (<2 percent) and the associated changes in cross-sectional area were ignored in the calculations. In experiments typified by curve B of Fig.2, the increase in slope at the yield point must be attributed to specimen deformation. For most applications, deformations as large as those displayed by curve B between the yield point and the failure point would be undesirable; therefore, for specimens typified by curve B, the ultimate compressive strength reported was calculated at the yield point ignoring specimen deformation occurring before the yield point. The data for both types of specimens were reduced in the same way, substituting the yield point for the failure point when the specimen exhibited yielding.

The hydrostatic support pressure at the failure point was obtained in the following manner. The hydrostatic support pressure at the contact point may be obtained from the apparatus calibration and the ram pressure at the contact point (P_c). The hydrostatic support pressure at the failure point was somewhat higher than at the contact point. Two factors enter into an estimate of this increase in support pressure. The first is an estimate of the advance of the pressure seal based on the compressibilities of the spacers and sealing piston. The second is an estimate of the increase in fluid pressure owing to the advance of the seal. Consideration of the ratio of the cross-sectional area of the spacers to the cross-sectional area of the pressure chamber indicates the rate of increase in fluid pressure per unit increase in piston advance to be decreased by a factor of seven compared to the rate before the contact point was reached. In this way a small incremental increase in applied ram pressure (ΔP) corresponding to the increased flu-

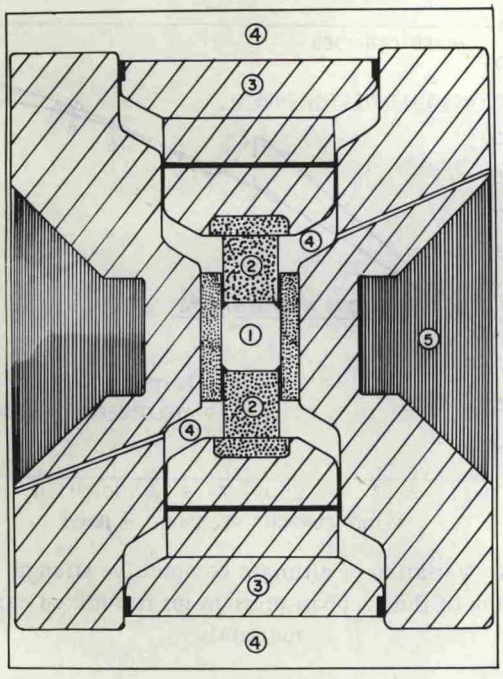

Fig. 6 Schematic representation of large volume high-pressure apparatus employing fluid enhancement of ultimate compressive strength of piston. Components are shown within chamber of a large autoclave: (1) sample, (2) fluid supported WC pistons, (3) driving piston, (4) hydrostatic fluid, and (5) lateral support mechanism

id pressure was estimated, and the hydrostatic support pressure at the failure point (σ_r) was taken to be the value corresponding to $P_c + \Delta P$ on the apparatus calibration curve.

The axial compressive stress on the specimen at failure was obtained by considering the ratio of the driving ram cross-sectional area to the specimen cross-sectional area (256:1). The ultimate compressive strength or axial compressive stress of the specimen at failure (σ_z) may thus be expressed as

$$\sigma_z = 256\ (P_u - P_c - \Delta P) + \sigma_r$$

where P_u is the applied ram pressure at the failure point or at the yield point for specimens which yielded before failure.

In this manner the experimental data, typified by the curves in Fig.2, were reduced to obtain the ultimate compressive strength (σ_z) as a function of hydrostatic support pressure (σ_r).

RESULTS AND DISCUSSION

The materials tested in these experiments were of three types: (1) Tungsten carbide with cobalt binder, (2) mixed carbides, and (3) oxide ceramics. The reduced data (σ_z versus σ_r) for the individual materials of each type are displayed in Figs.3, 4, and 5. The scatter of some of the data points was much too large to be attributed to the uncertainties of the measurement procedures and must be attributed to variations in the properties of the materials from specimen to specimen.

Tungsten Carbide with Cobalt Binder, Fig.3

These materials were purchased from the American Carbide Company in the final specimen configuration. The 3 percent cobalt binder, 6 percent cobalt binder, 13 percent cobalt binder, and 25 percent cobalt binder specimens were Amcarb grades D-5, D-20, D-40, and D-25, respectively. The specimens of tungsten carbide with 3 percent cobalt binder exhibited brittle failure at all support pressures tested, and the highest ultimate compressive strength observed was ~93 kbar with 14.1 kbar support pressure. The specimens of tungsten carbide with 6 percent cobalt binder exhibited varying degrees of yielding at all pressures. The amount of yielding was minimum near 6 kbar support pressure. The minimum in yielding is reflected by the hump in the σ_z versus σ_r curve near 6 kbar support pressure. The specimens of tungsten carbide with 13 percent cobalt binder also exhibited varying degrees of yielding. With zero support pressure slight yielding was observed. With approximately 3 kbar support pressure the specimens exhibited brittle fracture. With support pressures greater than 4 kbar, considerable yielding of the specimens and scatter in the data were observed. This variation in yielding produced a hump in the σ_z versus σ_r curve similar to that observed for the 6 percent cobalt binder specimens. The specimens of tungsten carbide with 25 percent cobalt binder yielded at all pressures. The amount of yielding increased with increasing support pressure.

Mixed Carbides, Fig.4

These materials were purchased from Metal Carbides Corporation in the final specimen configuration. The 65 percent tungsten carbide, 20 percent tantalum titanium carbide, 15 percent cobalt binder specimens were Talide grade CT-85. The 83 percent chrome carbide, 5 percent tungsten carbide, 12 percent nickel binder specimens were Talide grade CR-83. The tungsten-tantalum-titanium carbide specimens exhibited brittle failure at support pressures less than 6 kbar and yielded before failing at higher pressures. The low data point at 6.3 kbar support pressure was presumed

to be due to a faulty specimen. The σ_z versus σ_r curve for this material is similar to that for the tungsten carbide with 13 percent cobalt binder both in shape and the onset of yielding with higher pressures. The chrome-carbide specimen exhibited brittle failure at all pressures and the σ_z versus σ_r curve for this material is similar in shape to the curve for the tungsten carbide with 3 percent cobalt binder.

Oxide Ceramics, Fig.5

The specimens for these tests were cut from commercial stock in this laboratory. The Diamonite material was an aluminum-oxide ceramic with low percentage additives of chromium, magnesium, and silicon produced by the Diamonite Corporation. The Al_2O_3 material was a polycrystalline ceramic produced by Wesgo and reported to be 99.5 percent Al_2O_3. The Mullite material was a 3 Al_2O_3.2 SiO_2 ceramic produced by McDaniel, grade MY-30. The MgO material was a high-density ceramic, 99.5 percent MgO, produced by Minneapolis Honeywell. The Pyrex material was taken from the laboratory stock of unknown origin. Several other materials including $BaTiO_3$, Zircoa, sapphire, PZT, quartz, fired lava, and Corning Pyroceram were also tested. During the initial testing, these latter materials were observed to fail at pressures too low to justify further testing. As a group the oxide ceramics displayed very similar characteristics, all exhibiting essentially the same slope for the σ_z versus σ_r curves.

Overall, the most interesting feature of the data is the high ultimate compressive strength exhibited by the tungsten-carbide compounds with 13 percent cobalt binder when supported by only 3 kbar fluid pressure. Although we presently do not have a physical explanation for the anomalous characteristics of the 6 and 13 percent cobalt samples, these characteristics may be immediately employed in the design of high-pressure apparatus. With only 3 to 6 kbar fluid support pressure needed (instead of the usual 25 kbar), a double-piston arrangement similar to the Kennedy (3) apparatus could be constructed with considerable sample volume.

Fig.6 is a schematic representation of an alternate apparatus employing the fluid-enhancement scheme. This apparatus would operate within the pressure chamber of an autoclave, yielding a true "two stage" apparatus. The merit of the apparatus shown in Fig.6 lies in the economy of expanding the pressure range of relatively common autoclaves, rather than constructing a new press unit. The present technology of fluid-pressure-vessel design permits the manufacture of large internal diameter (125 cm) vessels (7) capable of containing pressures as high as 6 kbar. Employing the ultimate compressive strength enhancement exhibited by the carbides with around 13 percent cobalt binder, a piston-cylinder apparatus of considerable volume (on the order of thousands of cubic centimeters) and capable of pressures greater than 60 kbar could be constructed within such an autoclave.

REFERENCES

1 P. W. Bridgman, Proceedings, American Academy of Arts and Sciences, vol. 81, 1952, pp. 167-251.

2 H. T. Hall, Review of Scientific Instruments, vol. 29, 1958, p. 267.

3 P. N. La Mori, "High Pressure Measurement," Butterworths, London, England, 1963, p. 332.

4 P. W. Bridgman, "The Physics of High Pressure," G. Bell and Sons, 1958, p. 401.

5 P. W. Bridgman, "Studies in Large Plastic Flow and Fracture," Chapter 5, Harvard University Press, Boston, Mass., 1964.

6 Harwood Engineering, Walpole, Mass.

7 ASEA, (Allmanna Svenska Elektriska Aktiebolaget), Sweden, Bulletin 8146E.